ДГКС ASES | U-3
Kongres 2026
Congress 2026

doi: 10.67563/ASESCONF2026111T

Vesna Terzić[1]

RESILIENCE-BASED SEISMIC DESIGN: FROM THEORY TO ENGINEERING PRACTICE

Summary: Current seismic building codes aim to protect life safety by allowing controlled damage to lateral-load-resisting systems. Although this approach prevents collapse, buildings may remain unusable and impose significant consequences on communities and infrastructure. Resilience-based seismic design seeks to reduce these impacts, yet challenges remain in its practical application. This study examines one such challenge—the selection and availability of appropriate component fragility functions—through assessment of a modern 30-story reinforced-concrete core-wall building. Two models subjected to identical seismic demands are compared: a FEMA P-58 model using the closest available fragilities and a Custom model using component-specific fragilities derived from representative experimental data. Damage predictions are propagated through the F-Rec framework to evaluate functionality and recovery. Results demonstrate that practical application of existing resilience-assessment frameworks depends critically on the availability of reliable and appropriate component fragility functions.

Keywords: functional recovery, F-Rec framework, custom fragilities, tall building

ASEIZMIČKO PROJEKTOVANJE SA ASPEKTA OPORAVKA: OD TEORIJE DO INŽENJERSKE PRAKSE

Rezime: Važeći seizmički propisi za zgrade imaju za cilj zaštitu života ljudi dopuštanjem kontrolisanih oštećenja sistema za prijem horizontalnih opterećenja. Iako se ovakvim pristupom sprečava rušenje, zgrade mogu ostati neupotrebljive, uz značajne posledice po zajednicu i infrastrukturu. Seizmičko projektovanje zasnovano na sposobnosti oporavka (resilience-based seismic design) nastoji da smanji ove posledice, ali i dalje postoje izazovi u njegovoj praktičnoj primeni. U ovom istraživanju razmatra se jedan od tih izazova — izbor i dostupnost odgovarajućih funkcija fragilnosti komponenti — kroz procenu savremene tridesetospratne zgrade sa armiranobetonskim zidovima jezgra. Porede se dva modela izložena identičnim seizmičkim zahtevima: model FEMA P-58, u kojem su primenjene najsličnije dostupne funkcije fragilnosti, i prilagođeni model (Custom model), u kojem su korišćene funkcije fragilnosti specifične za pojedine komponente, izvedene na osnovu reprezentativnih eksperimentalnih podataka. Predviđena oštećenja dalje se obrađuju u okviru metodologije F-Rec radi procene funkcionalnosti i vremena oporavka. Rezultati pokazuju da praktična primena postojećih metodologija za procenu otpornosti i sposobnosti oporavka u presudnoj meri zavisi od dostupnosti pouzdanih i odgovarajućih funkcija fragilnosti komponenti.

Ključne reči: funkcionalni oporavak, metodologija F-Rec, prilagođene funkcije povredljivosti, visoka zgrada

[1] California State University Long Beach, USA, vesna.terzic@csulb.edu

1. INTRODUCTION

Over the past two decades, beginning with the development of the PEER performance-based earthquake engineering (PBEE) framework (described by Miranda and Aslani, 2003), substantial progress has been made toward resilience-based evaluation of individual buildings and building infrastructure. Comerio (2006) and Comerio and Blecher (2010) demonstrated that post-earthquake downtime includes not only physical repair but also delays associated with inspection, financing, engineering, permitting, and contractor mobilization, providing an empirical basis for subsequent impeding-factor and mobilization models. Cimellaro et al. (2010) formalized seismic resilience in terms of the loss and subsequent restoration of functionality over time. Mitrani-Reiser et al. (2012) advanced functional-loss assessment by relating structural and nonstructural damage and disruptions to utilities, equipment, supplies, and personnel to building functionality, while Mieler and Mitrani-Reiser (2018) synthesized the state of the art in earthquake-induced loss-of-functionality assessment and highlighted the broader consequences of building downtime.

FEMA P-58 (2012; revised 2018) established a standardized probabilistic methodology linking seismic demands to component damage and consequences, providing the component-level damage and repair information needed for subsequent recovery assessments. Its companion Performance Assessment Calculation Tool (PACT, 2012) enabled practical implementation of the methodology by integrating building information, engineering demands, component fragilities, and consequence functions to probabilistically estimate repair costs, repair times, casualties, and other losses. The subsequent development of the open-source NHERI-SimCenter Pelicun platform (Zsarnóczay et al., 2019) provided a flexible computational implementation of component-based probabilistic damage and loss assessment, facilitating FEMA P-58-type analyses and their integration with functional-recovery frameworks.

Building on these developments, REDi (Almufti and Willford, 2013) extended performance assessment toward resilience-based design by incorporating downtime, impeding factors, repair sequencing. Terzic and Yoo (2016) subsequently developed a building repair-time model incorporating realistic repair sequencing, labor allocation, concurrent-repair constraints, and resource availability. Terzic et al. (2021a,b) proposed F-Rec, the first probabilistic framework for building-level functional-recovery assessment that explicitly links component damage to system- and building-level functionality through fault-tree analysis and combines these functional dependencies with repair scheduling and mobilization time.

At the national level, NIST SP 1254/FEMA P-2090 (2021) established functional recovery as an explicit seismic-performance objective and provided recommendations for its incorporation into codes and standards. Building on existing concepts and methodologies, Molina Hutt et al. (2022) subsequently developed a probabilistic framework for evaluating temporal recovery to multiple performance states, including stability, shelter-in-place, reoccupancy, functional recovery, and full recovery. Finally, the integration of F-Rec with iRe-CoDeS in F-RecN+iRe-CoDeS (2023) extended detailed building-level recovery assessment to regional systems by incorporating infrastructure interdependencies and resource constraints. Collectively, these developments illustrate the evolution of PBEE from damage- and loss-based assessment toward explicit probabilistic evaluation of post-earthquake functionality and its recovery over time.

While significant advances have been made in developing frameworks and computational tools for resilience-based assessment of individual buildings, substantial challenges continue to limit their practical application. Among these, the availability and quality of component fragility functions remain particularly important. Fragility functions provide the fundamental link between engineering demand parameters and physical damage and, therefore, directly affect all subsequent predictions of functionality, repair requirements, recovery time, and economic loss. Despite their importance, experimentally validated fragilities remain scarce for many structural, architectural, and MEP components, particularly for modern or building-specific systems. Consequently, resilience assessments frequently rely on fragilities developed for components that only approximately represent those present in the building. Differences in component geometry, materials, detailing, installation, boundary conditions, and governing damage mechanisms, as well as the choice of EDP used to characterize demand, can result in substantially different damage predictions.

Similar limitations exist in consequence assessment. Reliable estimates of repair cost, repair duration, labor requirements, and functional impairment require consequence functions that appropriately represent each damage state and the specific building and regional context. These data are often even more limited than fragility data and can vary substantially with construction practices, labor and material availability, building occupancy, and local market conditions. Furthermore, translating physical damage into loss of functionality requires characterization of dependencies among structural and nonstructural components, building systems, and the services they provide. Such dependencies are highly building-specific and remain difficult to generalize.

Additional uncertainty arises from factors external to the building itself. Functional recovery can depend on the availability of power, water, telecommunications, transportation, and other lifeline services; access to contractors, specialized labor, equipment, replacement components, and financing; permitting, inspection, and regulatory processes; and the recovery of surrounding infrastructure and businesses. Broader socioeconomic conditions, including displacement of occupants, workforce availability, insurance and financing capacity, and competition for recovery resources, can further influence recovery. For major disasters, supply-chain disruptions, inflation, regional resource shortages, and broader economic or geopolitical conditions may also substantially affect the availability and cost of materials, equipment, and specialized services. These factors are inherently uncertain, spatially and temporally variable, and generally difficult to represent within current building-level resilience frameworks.

Thus, increasing the sophistication of recovery models alone does not necessarily improve the reliability of resilience predictions if the underlying damage and consequence models are not representative of the building being assessed. In particular, because component fragilities constitute the first link between calculated seismic demands and all subsequent damage, loss, and recovery calculations, inappropriate fragility selection can propagate through the entire assessment and substantially alter the predicted resilience of a building. This study focuses on this fundamental source of uncertainty by examining how the use of generic versus component-specific fragility functions affects predicted damage, functionality, and functional recovery of a modern tall building.

To investigate the influence of fragility representation on building resilience predictions, this study utilizes F-Rec framework to evaluate the seismic performance and functional recovery of a modern 30-story reinforced-concrete building using two alternative performance models. The first model uses the closest available component fragilities from the FEMA P-58 library, representing the approach commonly required when building-specific fragilities are unavailable, while the second incorporates component-specific fragilities developed from experimental data for systems representative of those installed in the building. Both models are subjected to identical seismic demands, allowing differences in predicted damage, functionality, and recovery time to be attributed directly to the adopted fragility representations. Particular attention is given to components for which the two models differ in the governing EDP, damage-state capacities, or underlying damage mechanisms, including reinforced-concrete walls, coupling beams, slab-column connections, window walls, and elevators. The resulting damage states are propagated through a functional-recovery analysis to quantify how differences at the component level affect system functionality, repair requirements, and ultimately building recovery. In this manner, the study demonstrates how differences introduced at the fragility-selection stage can propagate through the entire resilience-assessment process and materially influence conclusions regarding post-earthquake building performance. Finaly, the study identifies fragility development as a critical need for improving the reliability and practical applicability of resilience-based assessment.

2. FRAMEWORK FOR EVALUATION OF FUNCTIONAL RECOVERY OF A TALL BUILDING

Functional recovery of a 30-story residential building designed in accordance with the current building codes for a site in downtown Los Angeles is evaluated utilizing the novel probabilistic framework for modeling functional recovery, F-Rec framework (Terzic et al. 2021a; Terzic et al. 2021b; Terzic and Villanueva 2021). F-Rec framework is integrated into performance-based earthquake evaluation methodology (PBEE) (Miranda and Aslani 2003), as depicted in Figure 1.

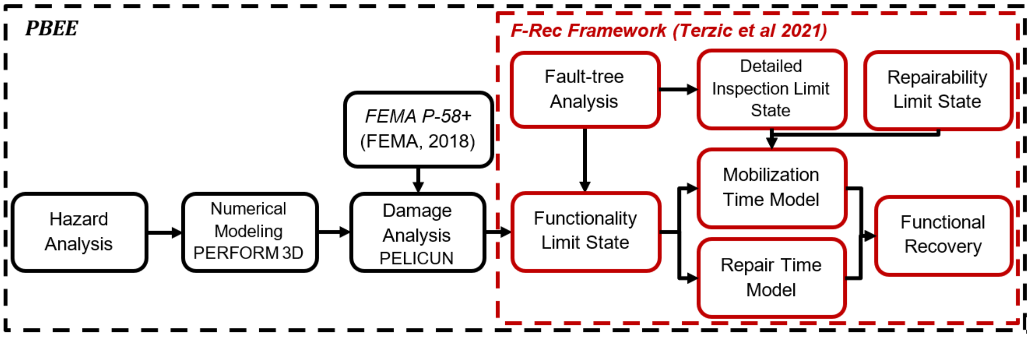

Figure 1: Framework for modeling functional recovery

The major outcome of the model is the recovery curve, which provides information on post-earthquake functionality (expressed as a percentage of the area within a building with preserved functionality), the total duration of recovery (i.e., recovery time), and path of recovery. The framework consists of three integrated moduli: 1) model for evaluation of post-earthquake functionality, 2) repair time model, and 3) mobilization time model. These three models are next described in more detail.

2.1. PROBABILISTIC MODEL FOR EVALUATION OF POST-EARTHQUAKE FUNCTIONALITY

A probabilistic building-level model for evaluation of post-earthquake functionality is essential for the proper estimation of the post-earthquake recovery process (Cimellaro et al. 2010; Burton et al. 2015; Terzic et al. 2016; Mieler and Mitrani-Reiser 2018; Sun et al. 2019). One such model, proposed by Terzic and Villanueva (2021), is incorporated in the F-Rec framework (Terzic et al. 2021a,b). The model is aligned with PBEE methodology and utilizes damage assessment results in conjunction with fault trees of complex building systems to find the percent of building area with compromised functionality. A generic fault tree, which relates the functionality of a complex building system to the state of its subsystems, is shown in Figure 2 (the term "Fails" means either full or partial (local) loss in building functionality). Furthermore, each subsystem has its fault tree that relates the damage state of its components to the functionality of the subsystem; an example of the subsystem fault tree is presented in Figure 3 for the HVAC system (see Terzic and Villanueva 2021 for other subsystems). To evaluate the functionality of building subsystems and the entire building through a fault-tree analysis, the model utilizes probabilistic limit state functions (LSFs) of individual building components as the primary user-defined inputs. These LSFs define the damage thresholds of components to partially (locally) and fully (globally) impair the building functionality.

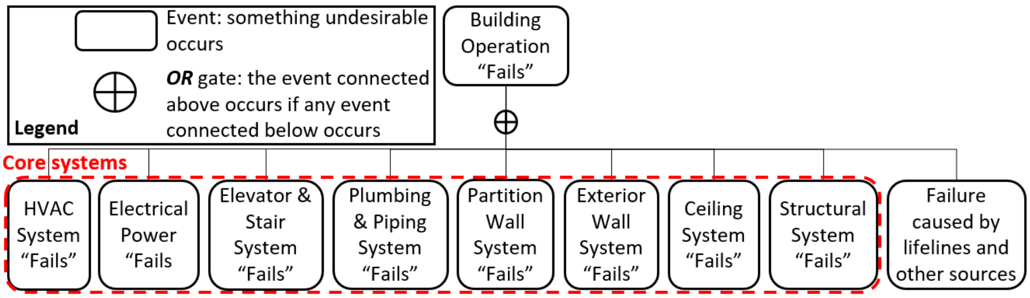

Figure 2: Generic fault tree for a complex building system (Terzic & Villanueva, 2021)

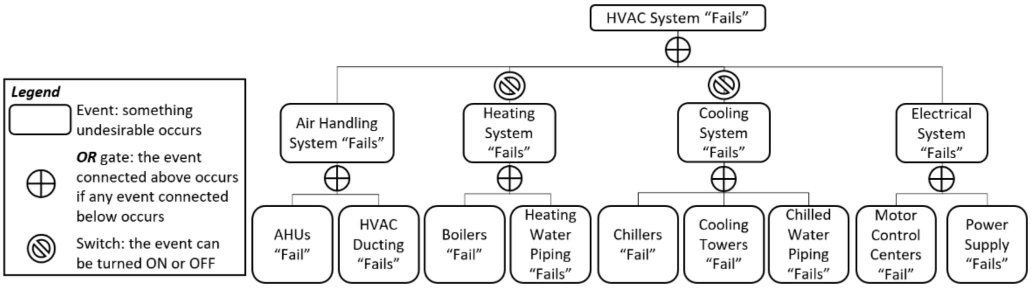

Figure 3: HVAC system fault tree (Terzic & Villanueva, 2021)

2.1.1. Functionality Limit State

In line with FEMA P-58 methodology, the information on damage states of all building components generated through the Monte Carlo process is utilized to explore the effect of uncertainty on the predicted loss of functionality. For each possible damage state of the building (i.e., a realization of the Monte Carlo simulation) the loss of functionality for the entire building is calculated following the procedure presented by Terzic and Villanueva (2021) and expressed with the following outcomes:

1. 0% loss of functionality, when all subsystems are fully functional;
2. X% (partial) loss of functionality (0 < X <100), when the function of some of the subsystems is compromised, while the rest of the building is open and functional; and
3. 100% loss of functionality, when any of the critical subsystems fail.

The functionality outcomes from all realizations are used to construct a post-earthquake functionality limit state, which is expressed as a probability that the "X" percent loss in functionality will be reached.

The unique features of the model are its capabilities to generate probabilistic post-earthquake functionality limit state for a particular earthquake scenario and to isolate building components that impair its functionality. The proposed model is highly flexible; it has a modular structure that allows easy extension and addition of new features.

2.2. REPAIR TIME MODEL

The Terzic et al. (2016) and Yoo (2016) repair time model (implemented in the F-Rec framework) was developed in collaboration with general contractors to realistically reflect current construction practices accounting for differences between new construction and repairing earthquake-induced damage. This repair time model, schematically presented in Figure 4, consists of two components: 1) *Repair Scheduling* that can accommodate any repair sequencing and considers realistic labor allocations, and 2) *Resource Scheduling*, which provides an efficient way of reducing workers during labor congestions while minimizing its prolonging effect on the project duration. The model considers sporadic spatial distribution of earthquake-induced damage at different floors of a building, the potential for the limited availability of the repair space that might slow down the repairs, and surge in construction demand that might impact large urban areas following a natural disaster.

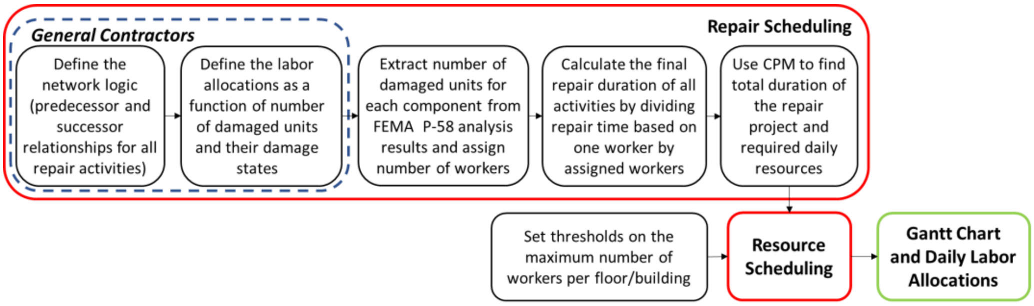

Figure 4: Repair time model for one realization of Monte Carlo simulation of FEMA P-58 assessment (Terzic et al. 2021a)

The repair scheduling method uses the logic network for a repair project, set by defining the predecessor/successor relationships and the number of floors repaired simultaneously for each repair activity, as well as labor allocations for different repair activities defined based on the severity and extent of damage to the building components; see Yoo (2016), Terzic et al. (2018), Terzic et al. (2020) for examples of logic networks and labor allocations generated in collaboration with general contractors. For every building component, the number of damaged units and their damage states are extracted from FEMA P-58 analysis results and used for labor allocations resulting in durations of repair activities. Repair durations of different damaged components are next used within the Critical Path Method (CPM) to find the total duration of the repairs and required daily labor resources. The outcomes of the method are the repair time fragility function, Gantt chart, and daily resource allocations for a selected realization.

2.3. MOBILIZATION TIME MODEL

The mobilization time model implemented in the F-Rec framework is an extension of the model proposed by Terzic et al. (2015). The model is based on Comerio's study (2006), complemented by FEMA 352 (FEMA, 2000) post-earthquake inspection strategies, and information collected from interviews with general contractors, building inspectors, structural engineers, and facility managers who were greatly involved in the recovery of Los Angeles following the 1994 Northridge earthquake. The flowchart shown in Figure 5 presents the adopted mobilization time model highlighting mobilization activities (shown blue) and their relationships based on the damage state of the building. The mobilization activities are modeled as lognormal functions to account for uncertainty associated with their durations that is dependent on socio-political factors, the economy, and the size and importance of the affected region. Median mobilization activities are defined by mobilization time functions that depend on many parameters including the severity of the damage, the number of damaged components in the building, relative contributions of structural and nonstructural damaged components to the overall damage, building's loss ratio, local economy, and importance and size of the building (all of these are presented in detail by Terzic et al. 2021a).

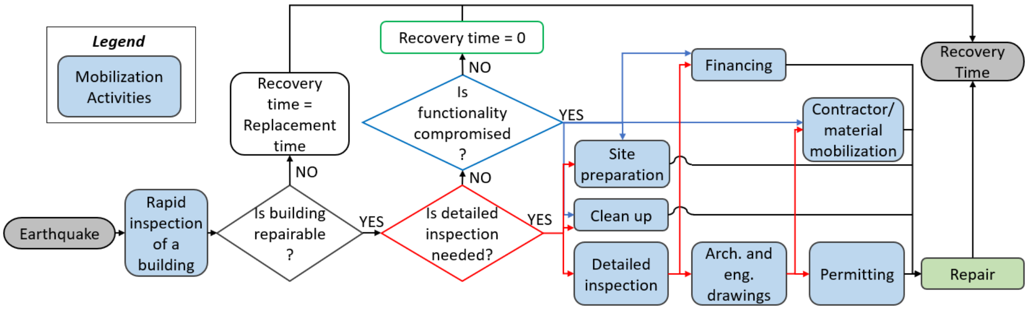

Figure 5: Schematic representation of the mobilization time model highlighting mobilization activities and their relationships based on the damage state of the building (Terzic et al. 2021a)

To support the calculation of mobilization time, as presented in Figure 5, it is necessary to evaluate three probabilistic limit state functions: repairability limit state (RLS), detailed inspection limit state (DILS), and functionality limit state (FLS). While FEMA P-58 provides a methodology for evaluation of RLS, Terzic and Villanueva (2021) propose the method for evaluation of FLS (a short description is provided in this paper) and Terzic et al. (2021a) propose a method for evaluation of DILS. Similar to FLS, DILS is developed by fault tree analysis, which utilizes information on structural and nonstructural damage of building components to evaluate if a detailed inspection is needed. The fault tree for the detailed inspection is derived from interviews with facility managers and building inspectors and is presented by Terzic et al. (2021a). A detailed inspection by structural engineers has typically been requested if a building has significant structural damage that would result in unsafe placard or if there is severe damage to nonstructural subsystems (e.g., piping, ceiling, exterior walls, and partition walls) that can hint of the presence of structural damage.

3. PERFORMANCE ASSESSMENT OF TALL RC CORE WALL BUILDING

3.1. BUILDING DESCRIPTION

The building is a 30-story residential building located in Los Angeles, California, recently designed by WSP Building Structures in accordance with LATBSDC (2023) performance-based seismic design methodology. The building consists of a core wall with coupling beams surrounded by concrete gravity columns and outrigger columns. In addition to 30-stories above ground, there are 4 basement levels of a parking structure surrounded by basement walls. Figure 6 shows the typical plan views of the basement levels and the typical above-grade floors from Stories 3 through 30. The first two floors of the building comprise the podium levels, which extend above grade from the basement structure.

In accordance with LATBSDC (2023) recommendations the building serviceability analysis was performed using a 43-year return period earthquake with 2.5% viscous damping. For the serviceability analysis, ductile elements (coupling beams for core wall building) were allowed to reach 150% of their capacity. The minimum strength was calculated based on the maximum of the 43-year return earthquake and wind loads. Subsequently, the building design was verified through nonlinear response-history analysis using a nonlinear finite element model developed in PERFORM-3D and Risk-Targeted Maximum Considered Earthquake (MCE) ground motions. Core wall shear, basement wall shear, and diaphragms were designed as force-controlled elements to remain essentially elastic under the MCE-level ground shaking. In addition, wall flexure and coupling beam shear behavior were treated as deformation-controlled components that are expected to experience nonlinear behavior, where nonlinear deformations of these components were all checked against appropriate limits.

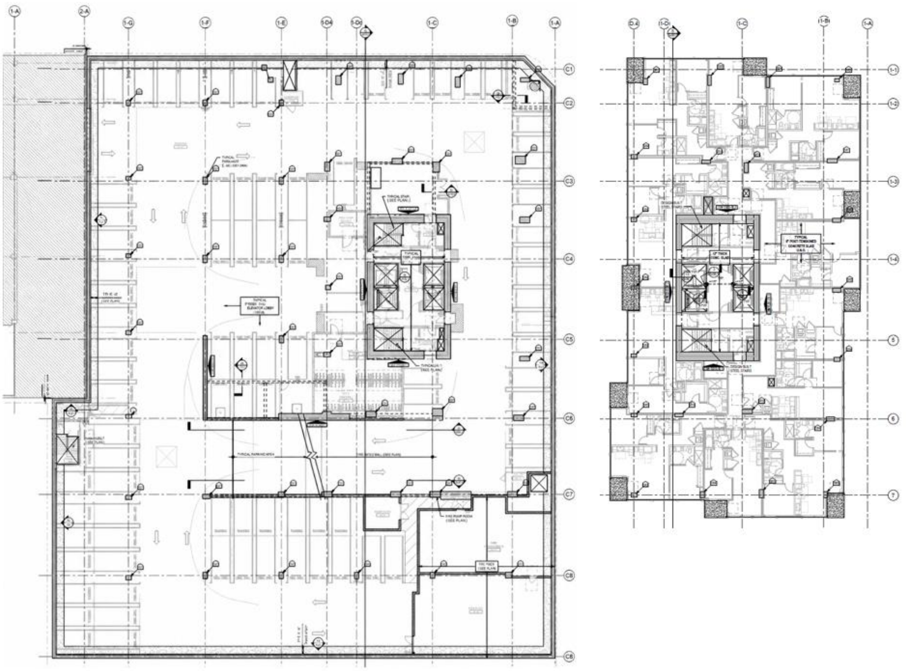

Figure 6: 30-story RC core-wall building: plan view of basement floors (left) and plan view of typical tower floors (right)

3.2. NONLINEAR ANALYSIS RESULTS

The analytical model of the building was subjected to a set of 11 ground motions representative of the MCE hazard level. The resulting building responses are presented in Figure 7 and include peak interstory drift ratios, peak floor accelerations, representative wall pier rotations, representative coupling beam (CB) rotations, and representative outrigger beam rotations. In addition, Table 1 presents the maximum residual interstory drift ratios (RID) obtained from the response-history analyses. Although several of these response quantities (i.e., floor acceleration, wall pier rotation, outrigger beam rotation) are not typically used as acceptance criteria in performance-based seismic design, they are used in this study as engineering demand parameters (EDPs) for evaluating component damage and the associated consequences (e.g., repair time and repair cost).

Results presented in Figure 7 show the median engineering demand parameter (EDP) and 90th percentile EDP. As observed from Figure 7, median peak interstory drifts (PID) for the MCE-level shaking are typically less than 2.5%, suggesting that the building overall deformation is within the limits used for the performance-based design of 3.0%. Interstory drifts in the X direction are approximately 25% larger than those in the Y direction, primarily due to the shorter length and resulting lower lateral stiffness of the reinforced concrete core in the X direction. The distribution of floor accelerations shows the largest values at the podium levels, followed by a relatively uniform response along the building height above the third story above grade. The analyses predicted median peak floor accelerations of less than 1.0g above the third story above grade and between 1.0g and 1.7g within the podium levels and below. Total wall pier rotations were relatively small, with median values ranging from 0.002 to 0.004 rad. Coupling beam rotation demands were generally larger in the Y direction, with the maximum median rotation reaching approximately 5.0%, below the 6.0% acceptance limit specified by the LATBSDC guidelines. Beams of outrigger system had median rotation typically less than 0.025 rad. Finally, interstory residual drifts (Table 1), obtained after sufficient free vibration of the building, averaged 0.588%, with a maximum value of 1.65%. The presented results are used as input for the recovery model described above to assess post-earthquake building functional recovery, which is discussed next.

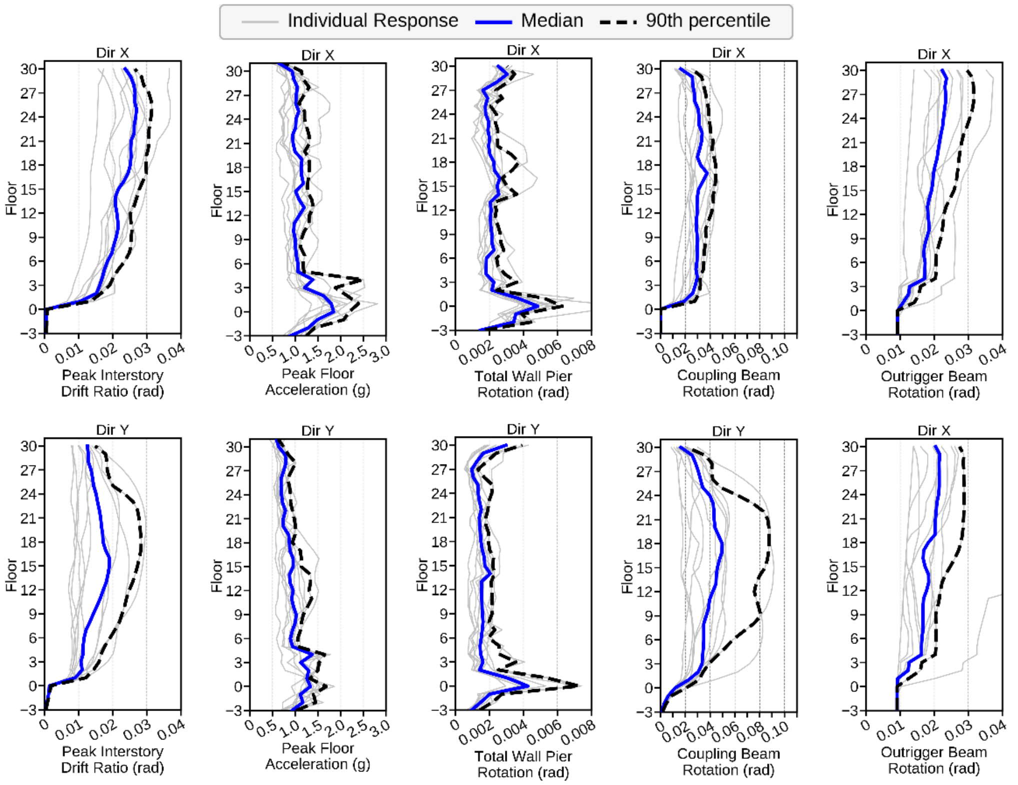

Figure 7: Engineering demand parameters: peak interstory drifts, peak floor accelerations, representative total wall pier rotations (other piers similar), representative coupling beam rotations (other locations similar), representative outrigger beam rotations (other locations similar)

Table 1: Residual Interstory Drifts (RID) obtained from nonlinear response-history analyses

Ground motion	GM1	GM2	GM3	GM4	GM5	GM6	GM7	GM8	GM9	GM10	GM11	Mean	Median	Max.
RID (%)	0.098	1.114	1.675	0.291	0.659	0.352	0.352	0.379	0.259	0.360	0.531	0.588	0.360	1.675

3.3. PERFORMANCE MODELING

Given that the primary objective of this study is to highlight the importance of component fragility functions in building resilience assessment, two performance models were developed: (1) a FEMA P-58 model, which used the closest available fragility functions from the FEMA P-58 fragility library to represent the building components; and (2) a Custom model, which incorporated custom fragility functions for components for which the FEMA P-58 library did not provide an exact or sufficiently representative match. Error: Reference source not found summarizes the component fragility functions that differ between the FEMA P-58 and Custom performance models. The custom fragility functions were derived from expanded or more recent experimental datasets relative to those underlying the corresponding FEMA P-58 fragilities or were developed specifically for components not represented in the FEMA P-58 library. The development and validation of these fragility functions are beyond the scope of this paper and will be presented in a separate publication.

Table 2: Comparison of FEMA P-58 and Custom fragility models

Component	Source	Fragility description	I/G	EDP	DS1	DS2	DS3
Slender walls/piers	FEMA P-58	Slender Concrete Wall	Grp.	Interstory Drift Max (rad)	0.00841 (0.51)	0.0123 (0.40)	0.189 (0.45)
	Custom	Slender Concrete Wall	Ind.	Total wall rotation (rad)	0.002 (0.209)	0.018 (0.415)	0.025 (0.407)
Coupling beams, aspect ratio < 2	FEMA P-58	Diagonally reinforced	Ind.	Chord Rotation (rad)	0.0179 (0.38)	0.0352 (0.44)	0.0543 (0.95)
	Custom	Diagonally reinforced	Ind.	Chord Rotation (rad)	0.013 (0.37)	0.033 (0.421)	0.055 (0.214)
Coupling beams, aspect ratio > 2	FEMA P-58	Diagonally reinforced	Ind.	Chord Rotation (rad)	0.0203 (0.39)	0.0394 (0.35)	0.0602 (1.00)
	Custom	Diagonally reinforced	Ind.	Chord Rotation (rad)	0.016 (0.38)	0.041 (0.442)	0.061 (0.337)
Slab-column connections of gravity columns	FEMA P-58	Post-tensioned concrete flat slab-column connections with shear reinforcing, 0 < Vg/Vo < 0.4	Grp.	Interstory Drift (rad)	0.028 (0.50)	0.040 (0.50)	-
	Custom	Post-tensioned concrete flat slab-column connections with shear reinforcing, 0 < Vg/Vn < 0.4	Grp.	Interstory Drift Max (rad)	0.035 (0.19)	0.053 (0.19)	-
Slab-column connections of outrigger columns	FEMA P-58	Post-tensioned concrete flat slab-column connections with shear reinforcing, 0 < Vg/Vo < 0.4	Grp.	Interstory Drift Max (rad)	0.028 (0.50)	0.040 (0.50)	-
	Custom	Outrigger beam-column connections within post-tensioned slab and with shear reinforcing, 0 < Vg/Vn < 0.4	Ind.	Total beam rotation (rad)	0.035 (0.19)	0.053 (0.19)	-
Window wall	FEMA P-58	Midrise stick-built curtain wall, 1-in. IGU tempered glass, 5 x 6 ft panels, 0.43-in. glass-to-frame clearance	Grp.	Interstory Drift Max (rad)	0.031 (0.25)	0.032 (0.25)	-
	Custom	Quest Ecowall 141 system, 1-in. IGU tempered glass, 4 x 12 ft panels, 0.75-in. head slip	Grp.	Interstory Drift Max (rad)	0.0432 (0.25)	0.0432 (0.25)	-
Traction elevator	FEMA P-58	Traction elevator - applies to most California installations, 1976 or later	Grp.	Peak Floor Acceleration (g)	0.39 (0.45)	-	-
	Custom	Otis SkyRise 1 Traction Elevator	Grp.	Residual Drift Interstory Drift COM (rad)	0.002 (0.20) 0.035 (0.20)	0.004 (0.20) -	- -

Note: DS = damage state; EDP = engineering demand parameter; I/G = individual/group (Grp. = group; Ind. = individual); COM = Center of Mass. Fragility values are reported as median (dispersion). A dash indicates that no value is specified.

The structural analysis results were incorporated into the two building performance models developed in NHERI-SimCenter Pelicun, an open-source probabilistic damage and loss assessment framework (Zsarnóczay et al., 2026). In addition to the component fragilities presented in Table 2, the performance models included appropriate fragility functions for the architectural, mechanical, electrical, and plumbing (MEP) components. The Monte Carlo simulation implemented in pelicun used 5,000 realizations to probabilistically characterize the range of potential building damage and associated consequences.

The types and quantities of structural components were extracted from the building drawings. Structural components represented in the performance models included slab-column connections, coupling beams, outrigger beams, and reinforced concrete shear walls. In the Custom model, each outrigger beam, coupling beam, and individual core wall pier was modeled separately, with element-specific EDPs assigned to capture variations in seismic demand throughout the building.

All major building equipment, including elevators, motor control centers, air-handling units, cooling towers, chillers, switchgear, transformers, and diesel generators, was modeled as anchored, with locations and quantities determined from the building drawings. Of particular importance, the Custom model incorporates elevator fragilities specifically developed to represent the Otis SkyRise 1 traction elevator system installed in the building. The modeled elevator damage mechanisms include guide-rail misalignment, derailment, and entrance-door jamming. Guide-rail misalignment and derailment are modeled as residual-interstory-drift-sensitive damage mechanisms, with fragility parameters derived from the guide-rail alignment and derailment tolerances applicable to the elevator system. Entrance-door jamming is modeled as an interstory-drift-sensitive damage mechanism, with the corresponding fragility developed using observations from the full-scale shake-table testing of a traction elevator reported by Wang et al. (2016).

Modern high-speed traction elevators incorporate seismic retainer plates designed to physically restrain the guide shoes relative to the rails and reduce the potential for complete derailment. In addition, counterweight displacement switches can stop elevator operation before excessive counterweight displacement results in a collision with the elevator car. Based on these protective features and the available experimental evidence, a separate fragility for earthquake-induced machinery damage was not included in the Custom model. In contrast, the FEMA P-58 elevator fragility is acceleration-sensitive and represents traction elevators installed in California in 1976 or later. The fragility was developed based on earthquake reconnaissance reports documenting elevator performance in low- and mid-rise hospital buildings and may therefore not adequately represent the damage mechanisms of modern high-speed traction elevators in tall buildings.

The types and quantities of exterior window walls, interior partition walls, and stairs were also determined from the building drawings. Because the specific window-wall system installed in the building is not represented in the FEMA P-58 fragility library, a custom fragility was developed based on the actual panel configuration. The glass-cracking damage state (DS1) was derived using the model proposed by O'Brien and Memari (2015), considering the dimensions, glass configuration, and available in-plane head slip of the installed window-wall system. Glass fallout (DS2) was conservatively assumed to occur at the same drift demand as glass cracking. Piping and ductwork quantities were estimated using the FEMA P-58 normative quantities for residential occupancy for all above-grade levels.

In Pelicun, each building component is associated with a fragility function that relates the applicable EDP to the probability of reaching or exceeding a specified damage state. In addition to component-level damage, Pelicun uses residual interstory drift to evaluate whether repair of the building is economically and technically feasible. Following FEMA P-58, the probability of demolition due to excessive residual drift is represented by a lognormal fragility function with a median residual drift ratio of 1.0% and logarithmic dispersion of 0.3. Consequently, sufficiently large residual drifts can trigger demolition in individual Monte Carlo realizations, resulting in consequences corresponding to full building replacement.

3.4. MODELING OF FUNTIONAL RECOVERY

Input data required to evaluate the functional recovery of the building using the proposed framework are specified for each of its three internal modules: functional loss state (FLS), repair time, and mobilization time.

As described previously, the calculation of FLS requires three primary inputs: (1) component damage states obtained from the damage analysis, (2) fault trees describing the functional dependencies among building systems and subsystems, and (3) limit-state functions (LSFs) that probabilistically define component damage thresholds associated with partial or complete loss of function. This case study utilizes the fault trees proposed by Terzic and Villanueva (2021), component damage states generated using Pelicun, and user-defined component LSFs based on Terzic and Kolozvari (2022). The FLS calculation does not account for the effects of external lifelines or other resources that may be critical to maintaining building functionality, such as utility services, critical building equipment, staff, and supplies, because sufficient data to characterize their post-earthquake availability were not available for this study.

Realistic estimation of repair time requires both a logical sequence of repair activities and appropriate allocation of labor resources. The repair schedule shown in Figure 8 and the labor allocations summarized in Table A1 (see Appendix section) were developed based on recommendations from contractors extensively involved in recovery efforts in the greater Los Angeles area following the 1994 Northridge earthquake. Figure 8 illustrates the principal dependencies among repair activities within and between floors.

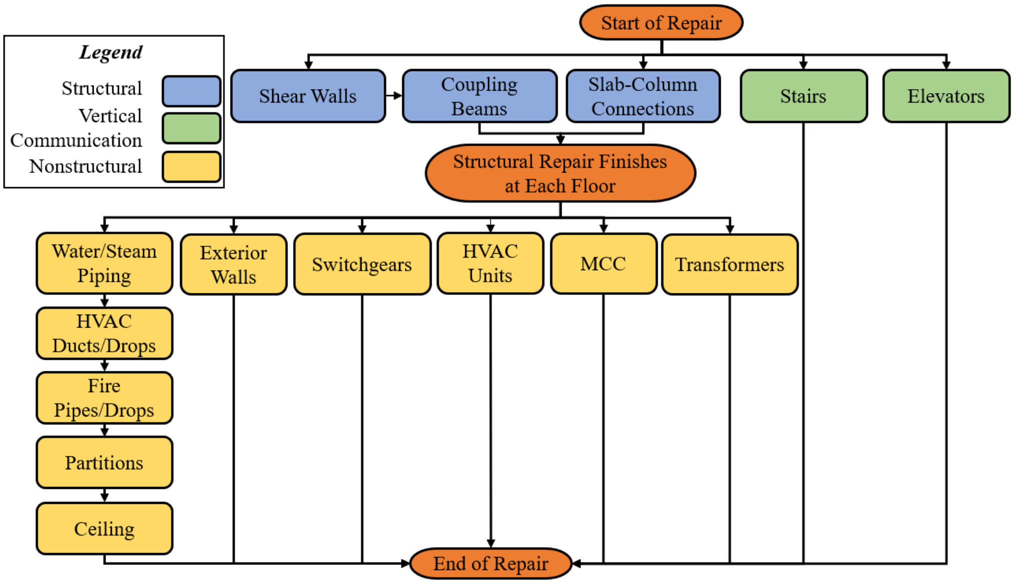

Figure 8: Flowchart of a realistic repair schedule for the 30-story building

Building repair begins with concurrent repair of structural components and vertical transportation systems (stairs and elevators), thereby restoring structural integrity while facilitating the movement of workers and materials. Repair of stairs and elevators is assumed not to constrain overall repair progress because temporary external construction elevators can be used when necessary. Structural repairs proceed from the bottom of the building upward, with repairs performed on up to four floors at a time. Nonstructural components are repaired sequentially, two floors at a time. Repair of a given nonstructural component on a floor is conditioned on both (1) completion of structural repairs on that floor and (2) completion of the same nonstructural repair activity on the floors below, allowing the corresponding repair crews to progress upward through the building.

Within each floor, concurrent repair is permitted for two groups of components: (1) interior finishes and distribution systems, including water and steam piping, HVAC ducts and drops, fire-suppression piping and drops, ceilings, and partitions; and (2) exterior enclosure components, including window walls. If structural damage is sufficiently severe to create unsafe occupancy conditions (e.g., issuance of an unsafe placard), repair of building equipment (i.e., Switchgear, HVAC Equipment, Motor Control Center (MCC), Transformer) is delayed until structural repairs are completed throughout the building. Otherwise, equipment repair is initiated at the beginning of the repair process. Labor allocations for the individual building components, commensurate with the extent of damage affecting building functionality, are summarized in Table A1.

Evaluation of mobilization time requires two primary types of input: (1) limit-state functions (LSFs) for nonstructural components (including piping, ceilings, exterior walls, and partition walls) that define damage thresholds for triggering detailed inspection; and (2) time allocations for individual mobilization activities. In this study, the median LSF threshold for all nonstructural components is set to 5%, such that severe damage to 5% of a given component type (e.g., partition walls) triggers a detailed inspection.

Time allocations for mobilization activities were established based on recommendations from general contractors, building inspectors, structural engineers, and facility managers involved in recovery efforts in the greater Los Angeles area following the 1994 Northridge earthquake and are summarized in Table A2. The assigned mobilization times depend on several damage and functionality attributes, including the type of damaged components affecting building functionality (e.g., equipment, nonstructural, or structural components), the component functionality state (full, partial, or no loss of function), the overall building functionality state (full, partial, or no loss of function), whether a detailed inspection is required, and the repair cost ratio expressed as a percentage of building replacement cost.

3.5. FUNCTIONAL RECOVERY COMPARISON BETWEEN CUSTOM MODEL AND FEMA P-58 MODEL

The structural response quantities obtained from the response-history analyses were incorporated into the two performance models to determine damage states of the building components. The resulting component damage was subsequently propagated through the F-Rec framework (Terzic et al., 2021a,b) to evaluate post-earthquake building functionality, mobilization, repair, and functional recovery. Because the Custom and FEMA P-58 models are subjected to the same structural demands and differ only in the fragility representation of selected components, differences in the resulting functionality and recovery predictions directly illustrate the influence of component fragility selection on resilience assessment. The recovery analysis considers only components whose damage is sufficient to impair building functionality.

Figure 9 compares the MCE functionality-state probabilities of the structural, exterior-wall, and elevator subsystems predicted by the two performance models. The most pronounced differences are observed for the structural and exterior-wall subsystems. For functionality impairment caused by structural damage, the Custom model predicts a 64% probability of full functionality loss, a 21% probability of partial loss, and a 15% probability of no loss. In contrast, the FEMA P-58 model predicts 100% probability of full functionality loss. Similarly, substantial differences are observed for the exterior-wall subsystem. The Custom model predicts an 86% probability of no functionality loss and only a 14% probability of partial loss, whereas the FEMA P-58 model predicts a substantially lower probability of no loss (38%) and a correspondingly higher probability of partial loss (62%). Both models predict a high probability of full functionality loss of the elevator system at the MCE hazard level. However, the Custom model also predicts a small probability that the elevators remain fully operational for ground motions producing negligible residual interstory drifts. These differences demonstrate the sensitivity of predicted building functionality to the fragility functions adopted in the performance model.

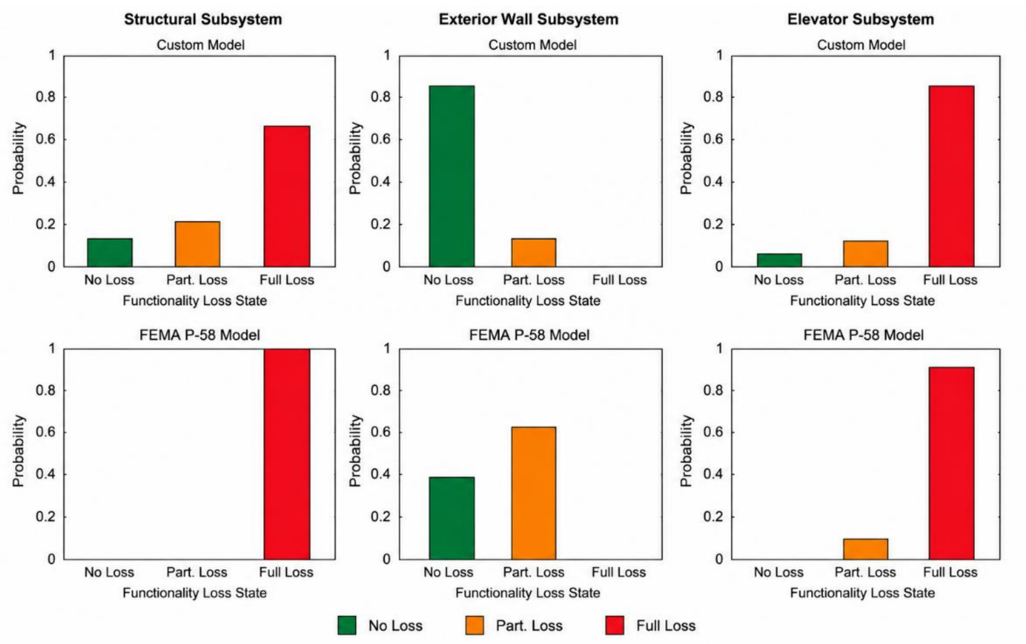

Figure 9: Subsystem Functionality Loss Comparison for the MCE hazard level between the Custom Model and FEMA P-58

The difference in structural-system functionality is primarily driven by the fragility representations of slender core-wall piers and slab-column connections. In the FEMA P-58 model, wall damage is evaluated using peak interstory drift, with median capacities of 1.23% and 1.89% for the functionality-impairing DS2 and DS3, respectively. Median interstory drifts exceeded the DS2 threshold over much of the building height and reached approximately 2.5%, resulting in widespread wall damage. In contrast, the Custom model evaluates individual wall piers using total wall rotation. Median rotations of 0.002–0.004 rad were well below the corresponding DS2 and DS3 capacities of 0.018 and 0.025 rad, resulting in substantially less functionality-impairing wall damage. Consequently, shear-wall repair is a major activity in the FEMA P-58 model but does not appear among the functionality-impairing repairs in the Custom model (Figure 11 and Figure 12).

Differences in the fragility functions for post-tensioned (PT) slab-column connections with shear reinforcement further contribute to the greater structural damage predicted by the FEMA P-58 model. The FEMA P-58 fragility, based on extrapolated experimental data for RC slabs, has median DS1 and DS2 drift capacities of 2.8% and 4.0%, whereas the Custom fragility, derived from experimental data for PT slabs, has higher capacities of 3.5% and 5.3%. The higher damage thresholds in the Custom model reduce both the frequency and severity of predicted slab-column connection damage.

A similarly pronounced difference in the exterior-wall subsystem results from the window-wall fragility representation. The FEMA P-58 model uses the closest available curtain-wall fragility, with median drift capacities of 3.1% and 3.2% for glass cracking and fallout, respectively. In contrast, the Custom model represents the actual Quest Ecowall 141 system, with a median drift capacity of 4.32% for both damage states. The higher drift capacity of the building-specific window-wall system results in substantially less predicted enclosure damage.

Although the effect of fragility selection on the elevator subsystem is less pronounced, it remains evident. The two models represent fundamentally different damage mechanisms: the FEMA P-58 model uses a single acceleration-sensitive fragility, whereas the Custom model represents guide-rail misalignment and derailment as residual-drift-sensitive mechanisms and entrance-door jamming as an interstory-drift-sensitive mechanism. Thus, despite relatively similar subsystem-level functionality probabilities at the MCE hazard level, the two models predict fundamentally different elevator damage mechanisms. Consequently, differences in predicted elevator functionality may become more pronounced at lower ground-motion intensities, where the probability of exceeding the respective fragility thresholds is lower.

These component-level differences propagate directly into the predicted functional recovery distributions shown in. In addition, although residual interstory drifts were relatively small for most realizations, a subset of outcomes exhibited large residual drifts (>1%), resulting in building replacement being triggered in 14% of the realizations due to excessive residual drift.. The Custom-model recovery distribution is shifted substantially toward shorter recovery times relative to the FEMA P-58 model. From the cumulative distributions, the median functional recovery time is 227 days for the Custom model and 385 days for the FEMA P-58 model, corresponding to an increase of roughly 160 days, or about 70%, when the FEMA P-58 fragility representation is used. The difference remains evident over much of the recovery-time distribution rather than being limited to a small number of realizations. In addition, although residual interstory drifts were relatively small for most realizations, a subset of outcomes exhibited large residual drifts (>1%), resulting in building replacement being triggered in 14% of the realizations due to excessive residual drift.

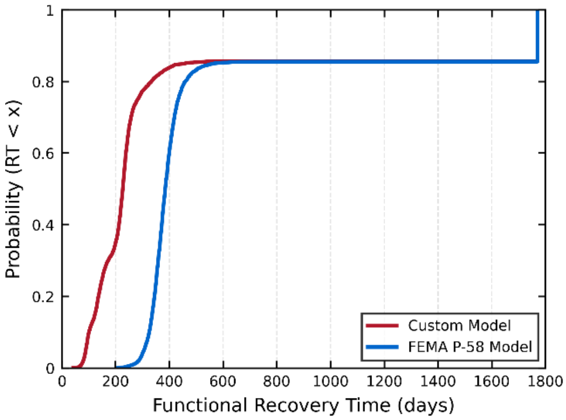

Figure 10: Functional recovery time fragilities for the two models: Custom and FEMA P-58 model

Figure 11 and Figure 12 provide further insight into the source of this difference by presenting the median MCE recovery trajectories, repair schedules, and mobilization durations for the Custom and FEMA P-58 models, respectively. In both models, the building experiences complete loss of functionality immediately following the earthquake. However, the subsequent recovery processes differ substantially. For the Custom model, functionality begins to recover after 124 days and is fully restored after 227 days. In contrast, the FEMA P-58 model begins recovering at approximately 155 days and does not achieve full functionality until 385 days.

The repair schedules show that this difference is driven primarily by the additional and more extensive structural repair requirements in the FEMA P-58 model. The Custom-model median repair schedule is governed primarily by coupling-beam repairs, while elevators, partitions, and RC slab-column connections at the top floor require comparatively shorter repair durations. In the FEMA P-58 model, shear-wall and PT slab-column connection repair become additional major repair activities that extend over a substantial portion of the building height. Because structural repair proceeds from the bottom upward and controls the initiation of dependent nonstructural repair activities, these additional structural repairs substantially delay restoration of building functionality.

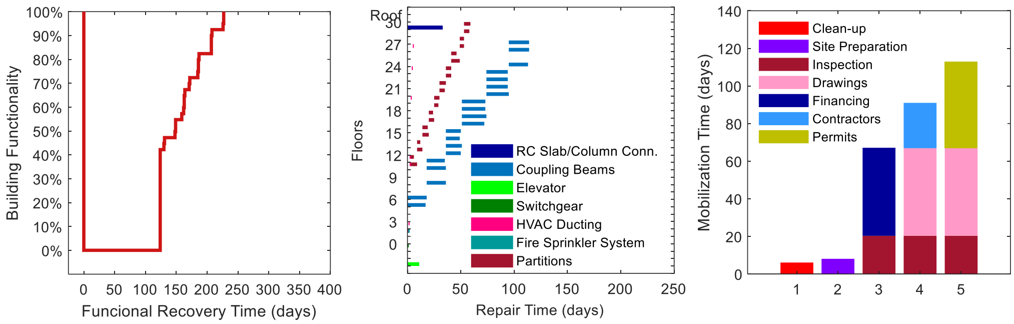

Figure 11: Median functional recovery evaluation results from Custom model for MCE hazard level: functional recovery curve, repair schedule, and time allocations of mobilization activities

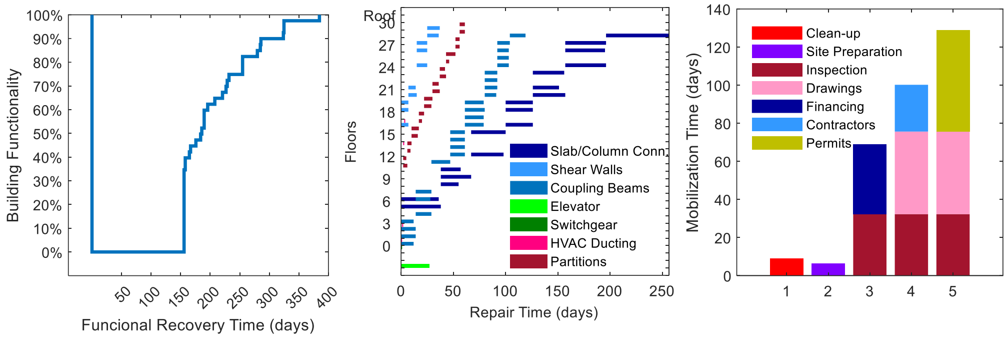

Figure 12: Median functional recovery evaluation results from FEMA P-58 model for MCE hazard level: functional recovery curve, repair schedule, and time allocations of mobilization activities

The two models also produce different mobilization requirements. The longest median mobilization sequence is 113 days for the Custom model and 130 days for the FEMA P-58 model. This 17-day difference is consistent with the greater amount of function-impairing damage and associated repair scope predicted by the FEMA P-58 model. Nevertheless, the difference in mobilization time is considerably smaller than the difference in total recovery time, indicating that the repair phase, particularly repair of structural components, is the dominant source of the model-to-model difference.

Overall, the comparison demonstrates that fragility-function selection can materially alter predicted building resilience even when the structural response demands are identical. The FEMA P-58 model predicts greater damage to the core walls, slab-column connections, and exterior enclosure, which results in higher probabilities of subsystem functionality loss and substantially longer repair and recovery times. In contrast, the Custom model uses component-specific fragilities and, where appropriate, element-specific EDPs that more directly represent the actual damage mechanisms of the building components. For the building considered herein, these differences reduce the median MCE functional recovery time by approximately 160 days relative to the FEMA P-58 representation. The results therefore demonstrate that using the closest available fragility from a generic library can introduce substantial bias into resilience estimates when the selected fragility does not adequately represent the component, its damage mechanism, or the EDP governing its response.

4. SUMMARY AND CONCLUSIONS

This study investigated the influence of component fragility representation on seismic resilience assessment of a modern 30-story reinforced-concrete core-wall building. Two performance models were developed and subjected to identical seismic demands: a FEMA P-58 model, which used the closest available fragility functions from the FEMA P-58 library, and a Custom model, which incorporated component-specific fragilities derived from experimental data representative of the systems present in the building. The resulting component damage states were propagated through the F-Rec framework to evaluate post-earthquake functionality, mobilization, repair, and functional recovery. This approach enabled the influence of fragility selection to be examined from the initial prediction of component damage through its consequences for building functionality and recovery.

The results demonstrate that differences in fragility representation can propagate from component-level damage predictions to substantially different estimates of building functionality and recovery. The largest differences were associated with the structural and exterior-wall subsystems. The Custom model predicted probabilities of full, partial, and no structural functionality loss of 64%, 21%, and 15%, respectively, whereas the FEMA P-58 model predicted 100% probability of full structural functionality loss. For the exterior-wall subsystem, the probability of no functionality loss increased from 38% with the FEMA P-58 model to 86% with the Custom model. These differences resulted primarily from the representation of slender core-wall piers, PT slab-column connections, and window walls. Differences in elevator functionality were less pronounced, although the two models represented fundamentally different elevator damage mechanisms.

The principal findings of this study are:

1. **Fragility representation can substantially affect predicted damage and functionality even when seismic demands are identical.** Differences in damage-state thresholds, governing EDPs, and component representation produced markedly different predictions, particularly for the structural and exterior-wall subsystems. The core-wall results illustrate the importance of the governing EDP: relatively high interstory drifts triggered widespread functionality-impairing wall damage in the FEMA P-58 model, whereas element-specific wall rotations remained well below the corresponding functionality-impairing thresholds in the Custom model.

2. **Differences in component damage propagate through the repair process and can have a disproportionate effect on functional recovery.** This is particularly important for structural components because their repair controls the progression of subsequent repair activities. In the FEMA P-58 model, predicted wall and PT slab-column connection damage resulted in their extensive repairs, whereas thier repair did not appear among the functionality-impairing activities in the median Custom-model repair schedule. Thus, differences introduced at the fragility level can ultimately alter both the activities controlling recovery and the time required to restore building function.

3. **Representative component fragilities are essential for reliable resilience assessment.** Generic fragility libraries provide an indispensable foundation when component-specific information is unavailable; however, the results demonstrate the limitations of using the closest available fragility when it does not adequately represent the component, its governing damage mechanism, or the appropriate EDP. Continued development and experimental validation of fragility and associated consequence functions for modern structural, architectural, and MEP systems are therefore critical for improving the reliability and practical applicability of resilience-based assessment.

Overall, the study demonstrates that the reliability of functional-recovery predictions depends not only on the sophistication of the recovery framework but also on the quality and relevance of the underlying component damage and consequence models. Improving the availability and quality of component fragility and consequence data is therefore a critical step toward translating resilience-based assessment from research into routine engineering practice.

ACKNOWLEDGEMENTS

The author gratefully acknowledges Siddharth Awasthi and Toni Ghodsi of WSP Building Structures, designers of the tall building analyzed in this study, for their valuable contributions and for providing extensive information essential to the functional-recovery assessment, including engineering demand parameters and detailed information on the types and quantities of structural, architectural, mechanical, and electrical components. The author also gratefully acknowledges Sofia Gavridou, Santiago Rodriguez, and Miki Mori for providing fragility functions for PT slab-column connections, wall piers, and coupling beams, respectively.

REFERENCES

Almufti I, Willford M (2013). Resilience-Based Earthquake Design Initiative for the Next Generation of Buildings (REDi Rating System). Arup, San Francisco, CA.

Blagojević N, Terzić V, Stojadinović B (2023). “F-RecN + iRe-CoDeS: Computational framework for regional recovery simulation using advanced building recovery models.” Engineering Structures, 288, 116156. https://doi.org/10.1016/j.engstruct.2023.116156.

Burton HV, Deierlein G, Lallemant D, & Lin T (2015), "Framework for incorporating probabilistic building performance in the assessment of community seismic resilience." Journal of Structural Engineering, Vol. 142, number 8.

Cimellaro GP, Reinhorn AM, & Bruneau M (2010), "Framework for analytical quantification of disaster resilience." Engineering Structures, Vol. 32, number 11.

Comerio MC (2006). “Estimating downtime in loss modeling.” Earthquake Spectra, Vol. 22, No. 2, pp. 349–365.

Comerio MC, Blecher HE (2010). “Estimating downtime from data on residential buildings after the Northridge and Loma Prieta earthquakes.” Earthquake Spectra, 26(4), 951–965. https://doi.org/10.1193/1.3477993.

Federal Emergency Management Agency (FEMA) (2000), “Recommended Post-Earthquake Evaluation and Repair Criteria for Welded Steel Moment-Frame Buildings,” FEMA 352, Washington, D.C.

Federal Emergency Management Agency (FEMA) (2012a). Seismic Performance Assessment of Buildings, Volume 1—Methodology, FEMA P-58-1. Washington, DC.

Federal Emergency Management Agency (FEMA) (2012b). Seismic Performance Assessment of Buildings, Volume 3—Performance Assessment Calculation Tool (PACT). Washington, DC.

Federal Emergency Management Agency (FEMA), 2018a, FEMA P-58-1: Seismic performance assessment of buildings, volume 1–methodology. Federal Emergency Management Agency, Washington, DC.

Los Angeles Tall Buildings Structural Design Council (LATBSDC) (2023). An Alternative Procedure for Seismic Analysis and Design of Tall Buildings. 2023 Edition. Los Angeles, CA.

Mieler MW and Mitrani-Reiser J (2018), “Review of the State of the Art in Assessing Earthquake-Induced Loss of Functionality in Buildings,” J. of Structural Engineering, Vol. 144(3).

Miranda E and Aslani H (2003). “Probabilistic response assessment for building specific loss estimation.” PEER Report 2003/03, Pacific Earthquake Engineering Research Center, University of California, Berkeley, CA.

Mitrani-Reiser J, Mahoney M, Holmes WT, de la Llera JC, Bissell R, Kirsch T (2012). “A functional loss assessment of a hospital system in the Bío-Bío Province.” Earthquake Spectra, 28(S1), S473–S502. https://doi.org/10.1193/1.4000044.

Molina Hutt C, Vahanvaty T, Kourehpaz P (2022). “An analytical framework to assess earthquake-induced downtime and model recovery of buildings.” Earthquake Spectra, 38(2), 1283–1320. https://doi.org/10.1177/87552930211060856.

National Institute of Standards and Technology (NIST) and Federal Emergency Management Agency (FEMA) (2021). Recommended Options for Improving the Built Environment for Post-Earthquake Reoccupancy and Functional Recovery Time, NIST SP 1254 / FEMA P-2090. https://doi.org/10.6028/NIST.SP.1254.

O’Brien WC, Memari AM (2015). “Prediction of seismic cracking capacity of glazing systems.” Earthquakes and Structures, 8(1), 101–132. https://doi.org/10.12989/eas.2015.8.1.101.

Sun L, Stojadinovic B, Sansavini G (2019), “Resilience Evaluation Framework for Integrated Civil Infrastructure–Community Systems under Seismic Hazard,” J. of Infrastructure Systems, Vol. 25(2).

Terzic V and Kolozvari K (2022). “Probabilistic evaluation of post-earthquake functional recovery for a tall RC core wall building using F-Rec framework.” Engineering Structures, 253, 113785. https://doi.org/10.1016/j.engstruct.2021.113785.

Terzic V and Villanueva PK (2021). “Method for Probabilistic Evaluation of Post-Earthquake Functionality of Building Systems,” Engineering Structures 241(15).

Terzic V, Kolozvari K, and Saldana D (2018). "Seismic Performance Assessment of Low- and Mid-Rise Office and Hospital Shear Wall Buildings," 16th European Conference in Earthquake Engineering, Thessaloniki, Greece, p. ID 10773.

Terzic V, Mahin SA, and Comerio MC (2015). “Using PBEE to Assess and Improve Performance of Different Structural Systems for Low-rise Steel Buildings,” Oral presentation, 2nd ATC-SEI Conference on Improving the Seismic Performance of Existing Buildings and Other Structures, San Francisco, CA.

Terzic V, Villanueva PK, Saldana D, and Yoo DY (2021a). “Framework for Modelling Post-Earthquake Functional Recovery of Buildings,” Engineering Structures 246(8).

Terzic V, Villanueva PK, Saldana D, and Yoo DY (2021b). “F-Rec Framework: Novel Framework for Probabilistic Evaluation of Functional Recovery of Building Systems,” PEER Report 2021/06, Pacific Earthquake Engineering Research Center, UC Berkeley.

Terzic V, Yoo D, and Aryan AH (2016). “Repair Time Model for Buildings Considering the Earthquake Hazard”, SEAOC Convention, Maui, HI.

Wang X, Hutchinson TC, Astroza R, Conte JP, Restrepo JI, Hoehler MS, Ribeiro W (2017). “Shake table testing of an elevator system in a full-scale five-story building.” Earthquake Engineering & Structural Dynamics, 46, 391–407. https://doi.org/10.1002/eqe.2793.

Yoo DY (2016), “Repair Time Model for Different Building Sizes Considering the Earthquake Hazard.” Master Thesis, California State University Long Beach, USA

Zsarnóczay A (2019). NHERI-SimCenter/pelicun: pelicun v2.0.0. Zenodo. https://doi.org/10.5281/zenodo.3491100.

Zsarnoczay A, Manousakis IV & Zhao J. (2026). NHERI-SimCenter/pelicun: v3.10 (Version v3.10). Zenodo. https://doi.org/10.5281/zenodo.21812989.

APPENDIX

Table A1: Workforce requirements for repair activities and functionality-impairing damage

A. Workforce per crew by ADS

Repair activity	ADS 0-1	ADS 1-2	ADS 2-3
Slab/column connections	4	6	N/A
Wall piers	4	6	8
Coupling beams	4	6	8
Stairs	2	3	4
Curtain walls	5	5	N/A

B. Number of crews based on NFIDU per floor

Repair activity	1-3	4-6	7-9	>12
Slab/column connections	1	2	3	4
Wall piers	1	2	3	4
Coupling beams	1	2	3	4
Stairs	1 crew if NFIDU < 2; 2 crews if NFIDU > 2			
Curtain walls	1 crew if NFIDU < 20; 2 crews if NFIDU > 20			

C. Total workforce for equipment that impairs function

Equipment	Workforce
Switchgear	2
Elevators	2
Chiller & cooling tower	3
AHUs	3
MCCs	3
Transformers	3

D. Total workforce based on RFIDU – nonstructural components

Component	0-0.1	0.1-0.5	0.5-1.0
Ceiling tiles (N/A)	2	5	9
HVAC ducting	1	3	5
Fire drops	1	2	3
Water piping	1	2	3

E. Total workforce based on RFIDU - partitions

Component	0-0.1	0.1-0.3	0.3-0.75	0.75-1
Partitions	2	5	11	15

Note: ADS = average damage state; RFIDU = ratio of functionality-impairing damaged units; NFIDU = number of functionality-impairing damaged units; N/A = not applicable.

Table A2: Median time allocation for mobilization activities by damaged-component type and functionality state

Mobilization Activity	**Type of damaged components that impair functionality**	**Functionality State**	**Median Time Allocation**
Detailed Inspection (DI)	Nonstructural only	Partial or full loss	1 week
	Structural	Partial loss	2 weeks
		Full loss	4 weeks
Architectural and Engineering Drawings	Nonstructural only	Full Loss + DI triggered	2 weeks
	Structural	Partial loss + DI triggered	3 weeks
		Full loss + DI triggered	6 weeks
Permitting	Nonstructural only	Full Loss + DI triggered	1 week
	Structural	Partial loss + DI triggered	3 weeks
		Full loss + DI triggered	6 weeks
Contractor and Material Mobilization	Equipment only	Partial loss & BF is partial loss	3 days
	Nonstructural only or with equipment	Partial loss & BF is partial loss	1 week
	Structural	Partial loss & BF is partial loss	2 weeks
	Equipment only	Full loss & BF is full loss	1 week
	Nonstructural only or with equipment	Full loss & BF is full loss	2 weeks
	Structural	Full loss & BF is full loss	3 weeks
Clean-up	Exterior walls, ceilings, partitions	Partial loss	1 week
		Full loss	2 weeks
Site Preparation	Equipment only	Full loss	0 days
	Structural and/or nonstructural	Full loss	1 week
Financing	Structural	Full loss & RCR>0.2	6 weeks
	Structural and/or nonstructural	Partial or full loss & RCR<0.2	2 weeks
	Equipment only	Partial or full loss	1 week

BF: building functionality; RCR: repair cost ratio as a percentage of replacement cost; DI: detailed inspection

Note: Dispersion of 0.2 is used for all activities